Toxicology in Vitro 48 (2018) 121–127

Contents lists available at ScienceDirect

Toxicology in Vitro

journal homepage: www.elsevier.com/locate/toxinvit

# The STIM1 inhibitor ML9 disrupts basal autophagy in cardiomyocytes by decreasing lysosome content

S. Shaikh[a], R. Troncoso[a,b], D. Mondaca-Ruff[a], V. Parra[a], L. Garcia[a], M. Chiong[a,*], S. Lavandero[a,c,**]

[a] Advanced Center for Chronic Disease (ACCDiS) & Center of Exercise, Metabolism and Cancer (CEMC), Faculty of Chemical & Pharmaceutical Sciences & Faculty of Medicine, University of Chile, Santiago, Chile
[b] Institute for Nutrition and Food Technology (INTA), University of Chile, Chile
[c] Department of Internal Medicine (Cardiology Division), University of Texas Southwestern Medical Center, Dallas, TX, USA

ARTICLE INFO

*Keywords:*
Autophagy
Cardiomyocytes
Cell death
LC3
ML9
Lysosomes

ABSTRACT

Stromal-interaction molecule 1 (STIM1)-mediated store-operated $Ca^{2+}$ entry (SOCE) plays a key role in mediating cardiomyocyte hypertrophy, both in vitro and in vivo. Moreover, there is growing support for the contribution of SOCE to the $Ca^{2+}$ overload associated with ischemia/reperfusion injury. Therefore, STIM1 inhibition is proposed as a novel target for controlling both hypertrophy and ischemia/reperfusion-induced $Ca^{2+}$ overload. Our aim was to evaluate the effect of ML9, a STIM1 inhibitor, on cardiomyocyte viability. ML9 was found to induce cell death in cultured neonatal rat cardiomyocytes. Caspase-3 activation, apoptotic index and release of the necrosis marker lactate dehydrogenase to the extracellular medium were evaluated. ML9-induced cardiomyocyte death was not associated with increased intracellular ROS or decreased ATP levels. Moreover, treatment with ML9 significantly increased levels of the autophagy marker LC3-II, without altering Beclin1 or p62 protein levels. However, treatment with ML9 followed by bafilomycin-A1 did not produce further increases in LC3-II content. Furthermore, treatment with ML9 resulted in decreased LysoTracker® Green staining. Collectively, these data suggest that ML9-induced cardiomyocyte death is triggered by a ML9-dependent disruption of autophagic flux due to lysosomal dysfunction.

## 1. Introduction

Depletion of intracellular $Ca^{2+}$ stores triggers a specialized $Ca^{2+}$ influx mechanism called store-operated $Ca^{2+}$ entry (SOCE) (Stathopulos and Ikura, 2017). SOCE is involved in replenishing $Ca^{2+}$ stores in the endoplasmic reticulum (ER) and sarcoplasmic reticulum (SR) (Stathopulos and Ikura, 2017). The major protein components of SOCE are the $Ca^{2+}$ sensor protein stromal-interaction molecule 1 (STIM1) and the $Ca^{2+}$ channel protein Orai1 (Zhang and Trebak, 2011).

STIM1 is mainly located in the ER but is also found in the plasma membrane and acidic stores. STIM1 contains a single transmembrane domain, an EF-hand domain, $Ca^{2+}$-binding and sterile alpha motif (SAM) domains in the ER/SR lumen, cytoplasmic ezrin-radixin-moesin (ERM) domains and Ser/Pro-rich and Lys-rich domains (Jardin and Rosado, 2016). STIM1 detects $Ca^{2+}$ depletion in the ER/SR and responds by clustering to ER/SR regions near the plasma membrane, where it activates the store-operated $Ca^{2+}$ channels Orai1 and TRPC1, allowing for $Ca^{2+}$ entry (Jardin and Rosado, 2016).

Several studies have described the presence and activity of SOCE in neonatal cardiomyocytes (Hunton et al., 2002; Uehara et al., 2002). Most of the evidence for the role of STIM1 in cardiomyocytes has been generated in the context of cardiac hypertrophy (Hulot et al., 2011; Luo et al., 2012; Voelkers et al., 2010). STIM1 is necessary for cardiomyocyte hypertrophy in vitro and in vivo (Hulot et al., 2011) as well as pathological cardiac hypertrophy (Luo et al., 2012). STIM1 also regulates normal and hypertrophic postnatal cardiac growth in vitro, along with Orai1 (Voelkers et al., 2010). Moreover, there is growing support for the contribution of SOCE to $Ca^{2+}$ overload, a key mediator of acute ischemia/reperfusion injury (Collins et al., 2013). Pharmacological

*Abbreviations:* ML9, 1-(5-chloronaphthalenesulfonyl) homopiperazine hydrochloride; STIM1, stromal-interacting molecule 1; GFP, green fluorescent protein; I/R, ischemia/reperfusion; LDH, lactate dehydrogenase; MTO, MitoTracker Orange; SOCE, store-operated $Ca^{2+}$ entry

* Corresponding author.
** Corresponding author at: Advanced Center for Chronic Disease (ACCDiS) & Center of Exercise, Metabolism and Cancer (CEMC), Faculty of Chemical & Pharmaceutical Sciences & Faculty of Medicine, University of Chile, Santiago, Chile
*E-mail addresses:* mchiong@uchile.cl (M. Chiong), slavander@uchile.cl (S. Lavandero).

https://doi.org/10.1016/j.tiv.2018.01.005
Received 4 November 2017; Received in revised form 6 January 2018; Accepted 9 January 2018
Available online 12 January 2018
0887-2333/ 

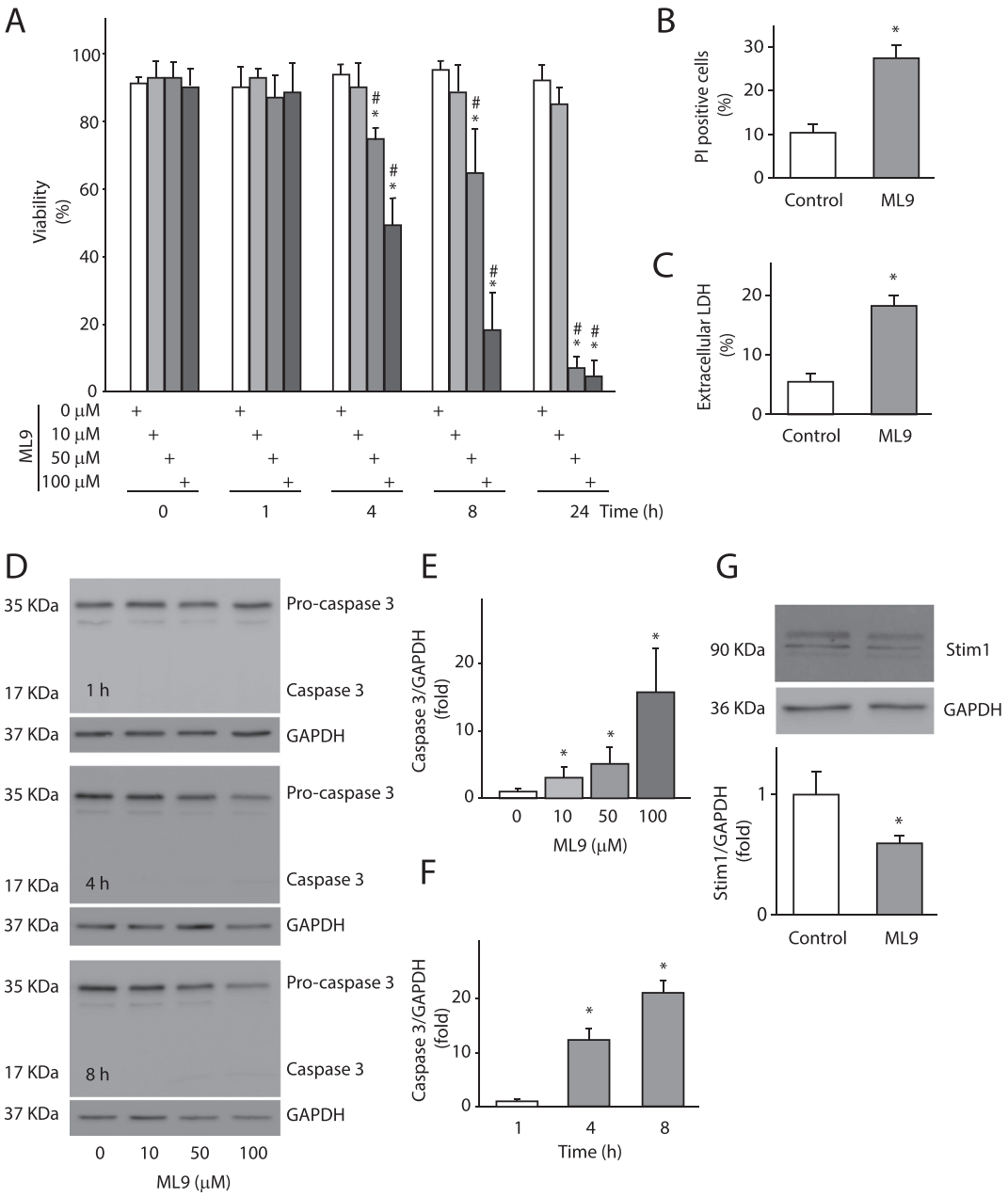


**Fig. 1.** ML9 induces cardiomyocyte cell death. (A) Dose dependent effects of ML9 on cardiomyocyte viability. Cultured NRVM were exposed to 0, 10, 50 and 100 μM ML9 for 0, 1, 4, 8 and 24 h. Cell viability was assessed by Trypan blue exclusion assay and is expressed as a percentage. Values are the mean of 6 independent experiments ± SEM. $^{*}p < 0.05$ vs. 0 h; $^{\#}p < 0.05$ vs. 0 μM ML9. (B–D) Induction cardiomyocyte necrosis by ML9. (B) Cultured NRVM were exposed to 50 μM ML9 for 4 h. Cells were trypsinized and stained with 10 μg/mL propidium iodide (PI) for 30 min at 37 °C and analyzed by flow cytometry. Values are the mean of 4 independent experiments ± SEM. $^{*}p < 0.05$ vs. control. (C) LDH activity was determined in the culture media by spectrophotometry. Values are the mean of 6 independent experiments ± SEM. $^{*}p < 0.05$ vs. control. (D-F) Induction cardiomyocyte apoptosis by ML9. Cultured NRVM were exposed to 0, 10, 50 and 100 μM ML9 for 1, 4 and 8 h. Total protein extracts were obtained and caspase-3 protein levels determined by Western blot. GAPDH was used as a loading control. (D) Representative Western blots. (E) Dose response of ML-9 on caspase 3 cleavage. (F) Time response of ML9 on caspase 3 cleavage. Values are the mean of 3 independent experiments ± SEM. $^{*}p < 0.05$ vs. respective control. (G) Regulation of STIM1 protein levels by ML9. Cultured NRVM were exposed to 50 μM ML9 for 4 h. STIM1 protein levels were determined by Western blot. GAPDH was used as a loading control. Upper panel is a representative Western blot. Lower panel is depicted in the quantification. Values are mean ± SEM. $^{*}p < 0.05$ vs. control.

inhibition of SOCE with $Gd^{3+}$, $La^{3+}$ and 2-aminoethoxydiphenyl borate abolishes $Ca^{2+}$ overload in adult mouse cardiomyocytes (Kojima et al., 2010). Glucosamine, a SOCE inhibitor, protects the heart against $Ca^{2+}$ overload and acute I/R injury (Liu et al., 2006). Therefore, STIM1 inhibition has been proposed as a therapeutic target for preventing cardiac hypertrophy and I/R-induced injury (Collins et al., 2013).

ML9 (1-(5-chloronaphthalenesulfonyl)homopiperazine hydrochloride) is a well-known chemical inhibitor of STIM1 (Smyth et al., 2008), Akt kinase (Garcia et al., 2005; Smith et al., 2000) and myosin light-chain kinase (Saitoh et al., 1987). However, little is known about the effects of ML9 on cardiomyocyte viability. To explore the use of ML9 as a potential therapeutic agent against cardiac hypertrophy and injury after I/R, we investigated the effects of ML9 on cardiomyocyte cell death. Surprisingly, we found that ML9 increases cardiomyocyte death by disrupting autophagy.

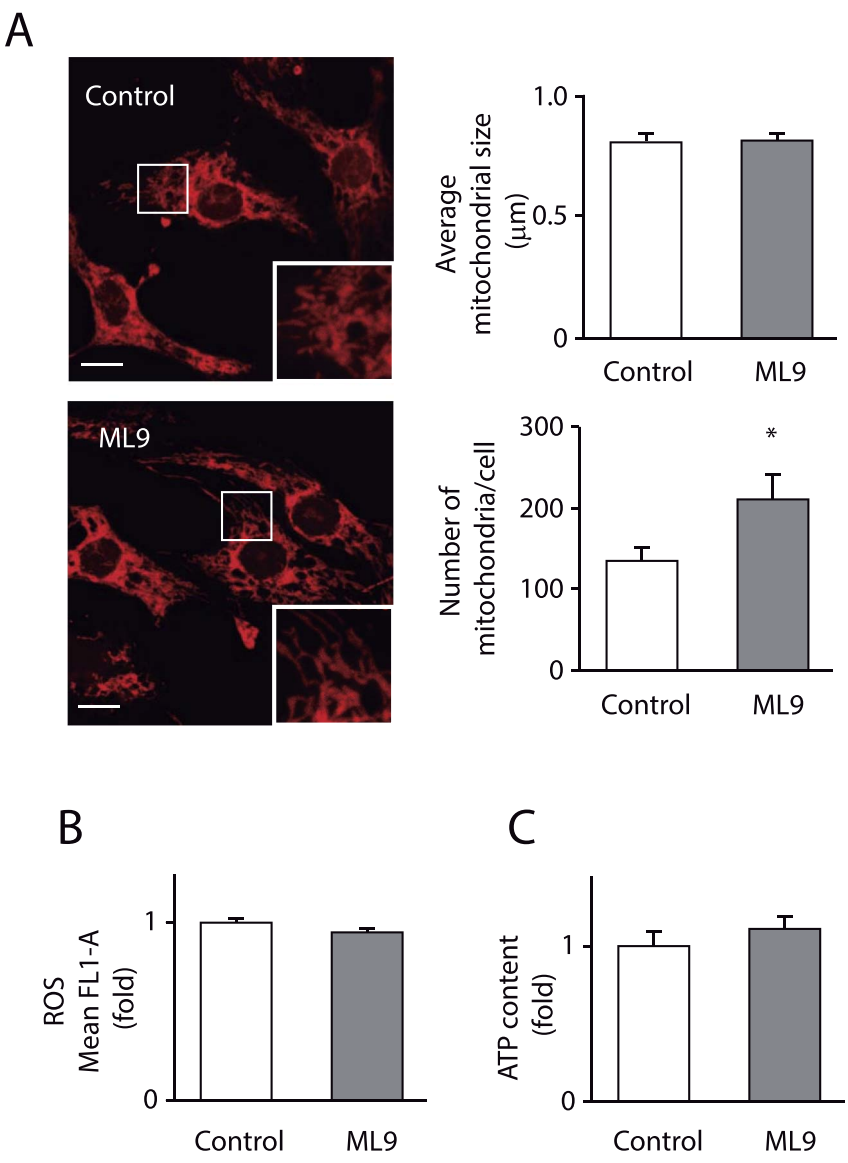


**Fig. 2.** ML9 does not modify cardiomyocyte mitochondrial morphology, ATP content or ROS levels.
(A) Mitochondria were labeled by preloading cultured NRVM with MitoTracker Orange (MTO, 200 nM) for 1 h. Then cells were exposed to 50 μM ML9 for 4 h. Z stack images were captured with confocal microscopy (60×). Inserts are amplifications of the indicated areas. Bar = 10 μm. After deconvolution, mitochondrial size and number were determined using Image J software. For each condition, at least 40 cells from 4 individual experiments were analyzed. Left panels are representative images. Right panels are the quantification. Values are the mean ± SEM of 4 independent experiments. *$p < 0.05$ vs. control. (B) Reactive oxygen species (ROS) production was measured with 2′,7′-dichlorofluorescin diacetate (DCFH-DA, 5 μM) using flow cytometry. Values are the mean ± SEM of 4 independent experiments. (C) ATP content was determined using luciferin/luciferase assay. Values are the mean of 6 independent experiments ± SEM.

## 2. Materials and methods

### 2.1. Reagents and antibodies

Fetal bovine serum (FBS), trypsin, and Hoechst were purchased from Invitrogen (CA, USA). ML9 was from Tocris Bioscience (MN, USA). Secondary antibodies were obtained from Calbiochem (ON, Canada). p62 antibody were from Abcam (MA, USA), and LC3, Beclin1, caspase-3, GAPDH, STIM1, secondary HRP-coupled antibodies were from Cell Signaling Technology (MA, USA). 2′,7′-dichlorofluorescin diacetate (DCFH-DA), MitoTracker Orange (MTO) and LysoTracker® Green was from Thermo Fisher Scientific (CA, USA). Non-fat milk was from Nestlé (Santiago, Chile). All materials for SDS-PAGE and Western blot, including PDVF membranes and ECL system, were from Bio-Rad Laboratories (CA, USA). DMEM, M199, bromodeoxyuridine, propidium iodide (PI) and all other reagents were analytical grade, purchased from Sigma-Aldrich Co. (MO, USA) or as specified in the corresponding manuscript section.

### 2.2. Cell culture

Rats were obtained from the Animal Breeding Facility of the University of Chile, Faculty of Chemical and Pharmaceutical Sciences. All experiments adhered to the Guide for the Care and Use of Laboratory Animals published by the U.S. National Institutes of Health (NIH) (8th Edition, 2011) and were approved by our Institutional Ethics Review Committee. Neonatal rat ventricular myocytes (NRVM) were isolated from 1 to 3-day-old Sprague-Dawley rat hearts. Lysates were digested with collagenase, and the resulting cell suspension was pre-plated to remove the fibroblasts. NRVM were plated at a density of 1250 cells/mm$^2$ in DMEM/M199 (4:1) media containing 10% FBS and 100 μM bromodeoxyuridine (Foncea et al., 2000). Cardiomyocytes were then cultured in DMEM 4.5 mg/mL glucose containing 2% FBS for at least 18 h prior to experiments.

### 2.3. Preparation of cell extracts and western blot analysis

After the corresponding experimental treatment, the culture medium was removed and the cells ($1.5 \times 10^6$) washed with cold PBS and scraped into 60 μL cold NP40 lysis buffer. Proteins were quantified by Bradford assay (Bio-Rad Laboratories, CA, USA). Proteins (approximately 30 μg/lane) were loaded and separated according to molecular weight by SDS-PAGE and transferred to PVDF membrane. Non-specific binding sites were blocked with 5% (*w/v*) non-fat milk in Tris-buffered saline (pH 7.6) containing 0.1% (v/v) Tween 20 for 1 h at room temperature. Membranes were incubated with the corresponding primary

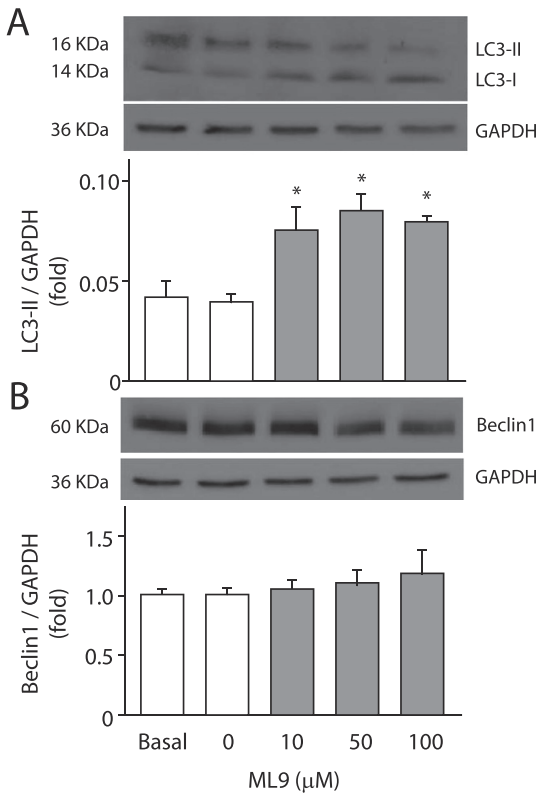


**Fig. 3.** ML9 increases LC3-II but not Beclin1 protein levels in cardiomyocytes. Cultured NRVM were exposed to 0, 10, 50 and 100 μM ML9 for 4 h. (A) LC3-II and (B) Beclin1 protein levels were determined by Western blot. GAPDH was used as a loading control. Upper panels are representative Western blots. Lower panels are the quantifications. Values are the mean ± SEM of 3 independent experiments. *$p < 0.05$ vs. basal levels.

antibodies overnight at 4 °C. GAPDH was used as a loading control in each experiment. After an additional incubation period with secondary HRP-coupled antibody for 1 h at room temperature, the blots were developed by chemiluminescence using the ECL system and quantified by scanning densitometry (Genesys, Syngene, USA).

### 2.4. Evaluation of necrosis and apoptosis

Cell death was quantified using PI staining. In brief, after the corresponding experimental treatment, the media were collected in tubes and the cells trypsinized and collected in the corresponding tube. Cells were stained with 10 μg/mL PI for 30 min at 37 °C and analyzed in the FL2-A channel of the flow cytometer (Accuri C6, BD Bioscience, USA). Data were analyzed using the BD CSampler platform. CytoTox 96® (Promega, WI, USA) is a non-radioactive, colorimetric assay. The assay measures lactate dehydrogenase (LDH), a stable cytosolic enzyme that is released upon cell lysis. Levels of LDH released into the culture media and total LDH were measured with coupled enzymatic assay (conversion of tetrazolium salt to red formazan). Visible wavelength (490 nm) absorbance data were recorded using a standard 96-well plate reader (Glomax Multidetection System, Promega, USA). Cleaved caspase-3 was used as an apoptotic marker, detected using Western blot.

### 2.5. Reactive oxygen species (ROS) production levels

To measure intracellular ROS levels, NRVM were grown over gelatin-coated culture plates. After the corresponding experimental treatment, cells were loaded with DCFH-DA (5 μM) for 30 min at 37 °C. The growth media were then collected in tubes and the cells trypsinized and collected in the corresponding tube. Cells were analyzed in the FL1-A channel of the flow cytometer (Accuri C6, BD Bioscience). Data were analyzed using the BD CSampler platform.

### 2.6. Mitochondrial and lysosomal analyses

Isolated cultured cardiomyocytes were subjected to experiment treatments, preincubated for 1 h with MTO (200 nM) and washed with Krebs solution. Cellular distribution of mitochondria was monitored using standard confocal microscopy with 60× magnification (Zeiss LSM 700, Germany). Images were analyzed with Image J (NIH, USA) software. For the lysosomal analysis, cardiomyocytes were cultured in DMEM supplemented with 2% serum for the basal autophagic condition. For the treatment condition, NRVM were incubated with 200 nM LysoTracker® Green for 1 h and then washed to remove excess probe. After treatment, the cells were washed with PBS and trypsinized. The collected cell suspensions were analyzed in the FL1-A channel of the flow cytometer.

### 2.7. ATP measurement

ATP content was determined by luciferin/luciferase assay (CellTiter-Glo Kit, Promega, USA).

### 2.8. Cell viability assay

Cell viability assays were performed using the trypan blue exclusion test as described (Copaja et al., 2011).

### 2.9. Evaluation of the progression of autophagy

The autophagosome-lysosome fusion suppressor bafilomycin-A1 was used to assess autophagy flux. Cultured NRVM were exposed to bafilomycin-A1 (50 nM) during the last 4 h of treatments. LC3 processing and p62 and Beclin1 levels were determined by Western blot (Klionsky et al., 2016). To assess autophagosome formation, cells were transduced with adenovirus expressing GFP-LC3 at a MOI of 20. Subcellular distribution of GFP-LC3 was monitored using standard confocal microscopy with 60× magnification (Zeiss LSM 700, Germany). Images were analyzed with Image J (NIH, USA) software.

### 2.10. Statistical analysis

Data are presented as mean ± SEM of n independent experiments and represent experiments performed on at least three separate attempts with similar outcomes. Data were analyzed using Student's t-test or ANOVA, and comparisons between groups were performed using a protected Dunnett's or Tukey's test; $p > 0.05$ was the cut-off for statistical significance. The GraphPad Prism 6 statistical program was used for data analysis.

## 3. Results

### 3.1. ML9 induces cardiomyocyte death

In cultured NRVM, increasing ML9 concentration and incubation time decreased cell viability. Basal cell death was 9 ± 2% and no reduction in cardiomyocyte viability was observed with 10 μM ML9 up to 24 h. However, treatment with 50–100 μM ML9 for 4–24 h significantly induced cell death (Fig. 1A). To characterize the type of cell death, NRVM were exposed to 50 μM ML9 for 4 h, which provoked a 2.5-fold increase in PI-positive cells over basal levels (Fig. 1B) and a 4-fold increase in extracellular LDH activity (Fig. 1C), suggesting necrotic cell death. However, 10–100 μM ML9 for 4–8 h also significantly increased cleaved caspase-3 levels (Fig. 1D–F), suggesting that ML9 also triggers cardiomyocyte apoptosis. The effectiveness of ML9 was verified by measuring STIM1 protein levels. Treatment with 50 μM ML9 for 4 h

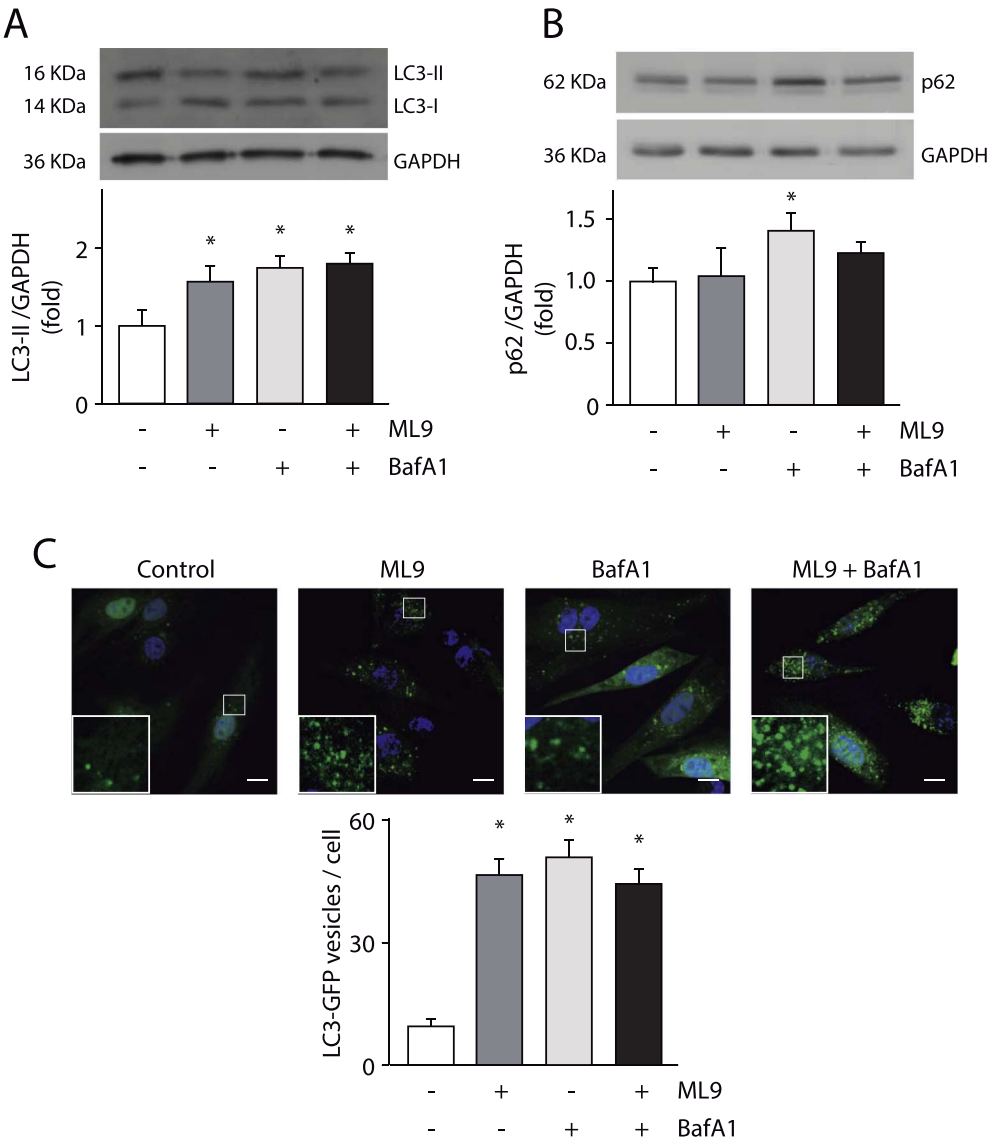


**Fig. 4.** ML9 disrupts autophagic flux in cardiomyocytes.
Cultured NRVM were exposed to 50 μM ML9 for 4 h in the presence or absence of bafilomycin A1 (BafA1, 50 nM). (A) LC3-II and (B) p62 protein levels were assessed by Western blot. GAPDH was used as a loading control. Upper panels are representative Western blots. Lower panels are the quantifications. Values are mean ± SEM of 3 independent experiments. *p < 0.05 vs. control. (C) Cultured NRVM were transduced with adenovirus overexpressing GFP-LC3 at a multiplicity of infection (MOI) of 20. After 24 h of culture, cardiomyocytes were exposed to 50 μM ML9 for 4 h in the presence or absence of bafilomycin A1 (BafA1, 50 nM). Images were acquired using confocal microscopy with 60× magnification and analyzed using Image J software. Inserts are amplifications of the indicated areas. Bar = 10 μm. LC3-GFP puncta were analyzed in 20 cells per experiment. Upper panels are representative images. Lower panels are the quantifications. Values are the mean ± SEM of 4 independent experiments. *p < 0.05 vs. basal levels.

decreased STIM1 protein levels by about 42% (Fig. 1G). Taken together, these results suggest that ML9 induces cardiomyocyte death through necrosis and apoptosis.

### 3.2. ML9 does not affect mitochondrial function in cardiomyocytes

To identify the mechanism underlying ML9-induced cardiomyocyte cell death, mitochondrial morphology and function were characterized. Treatment with 50 μM ML9 for 4 h increased the number of mitochondria per cell by about 63% over the basal condition (Fig. 2A). No changes were observed in mitochondrial size (Fig. 2A), ROS levels (Fig. 2B) or total ATP content (Fig. 2C). These results suggest that ML9 did not interfere with mitochondrial function. Therefore, energy metabolism is not likely to be involved in ML9-induced cell death.

### 3.3. ML9 disrupts autophagic flux in cardiomyocytes

We and others have shown that autophagy is required for cardiomyocyte survival under stress conditions (Lavandero et al., 2015; Marambio et al., 2010). To investigate whether autophagy is involved in ML9-induced cardiomyocyte death, levels of the autophagic markers LC3-II, Beclin1, p62 and autophagosomes were measured. Incubation with ML9 for 4 h increased total LC3-II protein in a concentration-dependent manner (Fig. 3A) but did not affect Beclin1 protein levels (Fig. 3B). Moreover, exposing cardiomyocytes to 50 μM ML9 for 4 h increased LC3-II levels by about 1.5-fold over control levels (Fig. 4A) but did not affect p62 protein levels (Fig. 4B). The above treatments also increased the number of autophagosomes, visualized as LC3-GFP puncta (Fig. 4C). Autophagic flux was assessed using bafilomycin-A1. Treatment with ML9 + bafilomycin-A1 produced no significant change in LC3-II levels as compared to ML9 alone (Fig. 4A), indicating that autophagic flux is inhibited by ML9. Moreover, p62 expression treatment was nearly identical after treatment with 50 μM ML9 vs. 50 μM ML9 + 50 nM bafilomycin-A1 (Fig. 4B). To confirm the above results, we analyzed autophagosome formation according to GFP-LC3 puncta distribution (Fig. 4C). Treatment with 50 μM ML9 vs. 50 μM ML9 + 50 nM bafilomycin-A1 produced similar levels of GFP-LC3 puncta formation (Fig. 4C). Taken together, these results suggest that ML9 inhibits autophagic flux in cardiomyocytes.

### 3.4. ML9 decreases lysosomal content in cardiomyocytes

To determine the mechanism underlying ML9-induced inhibition of autophagic flux, lysosomes were evaluated using LysoTracker® Green. This probe is a weakly basic amine that selectively accumulates in cellular compartments with low internal pH and is therefore often used

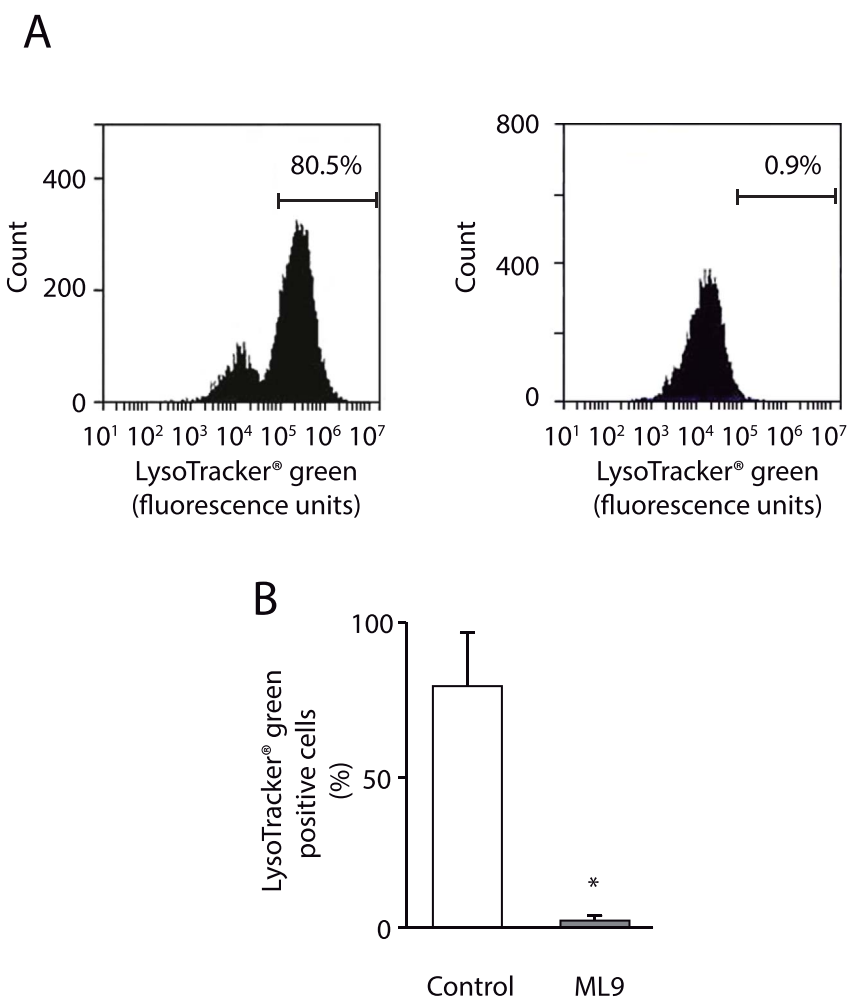


**Fig. 5.** ML9 decreases LysoTracker Green labeling in cardiomyocytes.
Cultured NRVM were exposed to 50 μM ML9 for 4 h. Lysosomes were labeled by incubating cardiomyocytes with 200 nM LysoTracker® Green during the last 1 h of ML9 treatment. Cells were detached using trypsin and analyzed using flow cytometry. Upper panels are representative cytometry histograms. Lower panel is the quantification. Values are the mean ± SEM of 3 independent experiments, each with 4 replicates. *$p < 0.05$ vs. control.

as a lysosome marker (Griffiths et al., 1988). Under basal conditions, > 80% of cardiomyocytes were stained with LysoTracker® Green (Fig. 5A). However, when cells were pretreated with 50 μM ML9, the LysoTracker® Green signal was almost null (Fig. 5B). This result suggests that ML9 affects lysosomes by increasing the pH of the compartment thereby decreasing the accumulation of LysoTracker® Green within the lysosomes.

## 4. Discussion

In this study, we provide compelling evidence that the STIM1 inhibitor ML9 induces cardiomyocyte death through necrosis and apoptosis by disrupting autophagic flux. ML9 induced necrosis at 4 h of treatment, as detected by increased incorporation of PI and release of LDH into the culture media. Moreover, at 8 h of ML9 treatment, cleaved caspase-3 levels were elevated, suggesting the occurrence of apoptosis. However, no alteration in ATP content, mitochondrial morphology or ROS production were detected, suggesting that neither energy collapse nor oxidative stress are likely to be involved in ML9-induced cardiomyocyte death.

Previous reports regarding the effects of ML9 on cell death have been contradictory. ML9 induces apoptosis in normal and transformed MCF-10A epithelial cells (Connell and Helfman, 2006) and in LNCaP prostate cancer cells (Kondratskyi et al., 2014). This effect has been linked to myosine light chain kinase (MLCK) inhibition (Connell and Helfman, 2006; Kondratskyi et al., 2014). Here, we found that ML9 triggers apoptosis and necrosis in NRVM. To our knowledge, this is the first description of ML9-triggered necrosis. However, ML9 does not induce apoptosis in clonal neuronal cells from the cell line ML-DmBG2-c2, derived from the central nervous system of Drosophila larvae (Nagano et al., 1998). Furthermore, ML9 has an antiapoptotic action in endothelial progenitor cells (Wang et al., 2016) and PC12 cells (Li et al., 2013). In these last two cases, the effects of ML9 have been linked to STIM1 inhibition (Li et al., 2013; Nagano et al., 1998). Therefore, the effect of ML9 on viability is cell type-dependent. So far, ML9 metabolites have not been described. Therefore, we cannot discard that some of the contradictory data could be due to toxic effect of ML9 metabolites rather than ML9 itself.

Autophagy is a predominantly protective mechanism against disease-related stress, but dysfunctional or impaired autophagy may contribute to the morbidity and mortality associated with cardiovascular diseases (Lavandero et al., 2015). We have previously described that inhibition of autophagy in stressed cardiomyocytes promotes cell death (Marambio et al., 2010). Moreover, proper control of autophagic flux supports cardiomyocyte viability (Troncoso et al., 2012). Therefore, ML9-induced disruption of autophagy disruption may be an important trigger for cardiomyocyte death.

Previous evidence has shown that ML9 can disrupt autophagic flux. Zhang et al. (Zhang et al., 2007), using high-throughput, image-based screening for small-molecule regulators of autophagy, found that ML9 increases the number of GFP-LC3 vesicles in human glioblastoma H4 cells. Moreover, a structurally-related analog of ML9 known as ML7 induces accumulation of vesicle-like structures in Schwann cells (Leitman et al., 2011). Kondratskyi et al. (Kondratskyi et al., 2014) described that ML9 induces the accumulation of autophagic vacuoles in prostate cancer cells. Here, we showed that ML9 also induces

accumulation of GFP-LC3-positive vesicles in cardiomyoctyes. Our data suggest that the ML9-induced increase in GFP-LC3 vesicles is due to inhibition of autophagosome degradation. Kondratskyi et al. (Kondratskyi et al., 2014) proposed that this effect of ML9 may be attributable to its weak base properties. ML9, as a lipophilic weak base, may enter the cell by simple diffusion. At a neutral pH, ML9 should be in its non-protonated form. When ML9 enters an acidic vacuole such as a lysosome, it is protonated, becoming positively charged and therefore trapped in the organelle. This sequence of events should lead to an increase in intralysosomal pH, inhibiting the lysosomal enzymes and disrupting autophagy.

Given its effects on cardiomyocyte viability and autophagy, our results suggest that ML9 would not be useful a cardioprotector during ischemia/reperfusion nor as an anti-hypertrophic compound. However, in vivo research should be performed to corroborate our findings.

## Conflict of interest

The authors declare that there is no conflict of interest.

## Transparency document

The Transparency document associated with this article can be found, in online version.

## Acknowledgements

This work was supported by a grant from FONDECYT, Chile (Postdoctoral Fellowship 3150545 to S. Shaikh) and FONDAP 15130011 (to S.L., M.C., L.G., V.P. and R.T.).

## References

Collins, H.E., Zhu-Mauldin, X., Marchase, R.B., Chatham, J.C., 2013. STIM1/Orai1-mediated SOCE: current perspectives and potential roles in cardiac function and pathology. Am. J. Physiol. Heart Circ. Physiol. 305, H446–458.

Connell, L.E., Helfman, D.M., 2006. Myosin light chain kinase plays a role in the regulation of epithelial cell survival. J. Cell Sci. 119, 2269–2281.

Copaja, M., Venegas, D., Aranguiz, P., Canales, J., Vivar, R., Catalan, M., Olmedo, I., Rodriguez, A.E., Chiong, M., Leyton, L., Lavandero, S., Diaz-Araya, G., 2011. Simvastatin induces apoptosis by a rho-dependent mechanism in cultured cardiac fibroblasts and myofibroblasts. Toxicol. Appl. Pharmacol. 255, 57–64.

Foncea, R., Galvez, A., Perez, V., Morales, M.P., Calixto, A., Melendez, J., Gonzalez-Jara, F., Diaz-Araya, G., Sapag-Hagar, M., Sugden, P.H., LeRoith, D., Lavandero, S., 2000. Extracellular regulated kinase, but not protein kinase C, is an antiapoptotic signal of insulin-like growth factor-1 on cultured cardiac myocytes. Biochem. Biophys. Res. Commun. 273, 736–744.

Garcia, B.G., Wei, Y., Moron, J.A., Lin, R.Z., Javitch, J.A., Galli, A., 2005. Akt is essential for insulin modulation of amphetamine-induced human dopamine transporter cell-surface redistribution. Mol. Pharmacol. 68, 102–109.

Griffiths, G., Hoflack, B., Simons, K., Mellman, I., Kornfeld, S., 1988. The mannose 6-phosphate receptor and the biogenesis of lysosomes. Cell 52, 329–341.

Hulot, J.S., Fauconnier, J., Ramanujam, D., Chaanine, A., Aubart, F., Sassi, Y., Merkle, S., Cazorla, O., Ouille, A., Dupuis, M., Hadri, L., Jeong, D., Muhlstedt, S., Schmitt, J., Braun, A., Benard, L., Saliba, Y., Laggerbauer, B., Nieswandt, B., Lacampagne, A., Hajjar, R.J., Lompre, A.M., Engelhardt, S., 2011. Critical role for stromal interaction molecule 1 in cardiac hypertrophy. Circulation 124, 796–805.

Hunton, D.L., Lucchesi, P.A., Pang, Y., Cheng, X., Dell'Italia, L.J., Marchase, R.B., 2002. Capacitative calcium entry contributes to nuclear factor of activated T-cells nuclear translocation and hypertrophy in cardiomyocytes. J. Biol. Chem. 277, 14266–14273.

Jardin, I., Rosado, J.A., 2016. STIM and calcium channel complexes in cancer. Biochim. Biophys. Acta 1863, 1418–1426.

Klionsky, D.J., Abdelmohsen, K., Abe, A., Abedin, M.J., Abeliovich, H., et al., 2016. Guidelines for the use and interpretation of assays for monitoring autophagy (3rd edition). Autophagy 12, 1–222.

Kojima, A., Kitagawa, H., Omatsu-Kanbe, M., Matsuura, H., Nosaka, S., 2010. Ca2+ paradox injury mediated through TRPC channels in mouse ventricular myocytes. Br. J. Pharmacol. 161, 1734–1750.

Kondratskyi, A., Yassine, M., Slomianny, C., Kondratska, K., Gordienko, D., Dewailly, E., Lehen'kyi, V., Skryma, R., Prevarskaya, N., 2014. Identification of ML-9 as a lysosomotropic agent targeting autophagy and cell death. Cell Death Dis. 5, e1193.

Lavandero, S., Chiong, M., Rothermel, B.A., Hill, J.A., 2015. Autophagy in cardiovascular biology. J. Clin. Invest. 125, 55–64.

Leitman, E.M., Tewari, A., Horn, M., Urbanski, M., Damanakis, E., Einheber, S., Salzer, J.L., de Lanerolle, P., Melendez-Vasquez, C.V., 2011. MLCK regulates Schwann cell cytoskeletal organization, differentiation and myelination. J. Cell Sci. 124, 3784–3796.

Li, X., Chen, W., Zhang, L., Liu, W.B., Fei, Z., 2013. Inhibition of store-operated calcium entry attenuates MPP(+)-induced oxidative stress via preservation of mitochondrial function in PC12 cells: involvement of Homer1a. PLoS One 8, e83638.

Liu, J., Pang, Y., Chang, T., Bounelis, P., Chatham, J.C., Marchase, R.B., 2006. Increased hexosamine biosynthesis and protein O-GlcNAc levels associated with myocardial protection against calcium paradox and ischemia. J. Mol. Cell. Cardiol. 40, 303–312.

Luo, X., Hojayev, B., Jiang, N., Wang, Z.V., Tandan, S., Rakalin, A., Rothermel, B.A., Gillette, T.G., Hill, J.A., 2012. STIM1-dependent store-operated Ca(2)(+) entry is required for pathological cardiac hypertrophy. J. Mol. Cell. Cardiol. 52, 136–147.

Marambio, P., Toro, B., Sanhueza, C., Troncoso, R., Parra, V., Verdejo, H., Garcia, L., Quiroga, C., Munafo, D., Diaz-Elizondo, J., Bravo, R., Gonzalez, M.J., Diaz-Araya, G., Pedrozo, Z., Chiong, M., Colombo, M.I., Lavandero, S., 2010. Glucose deprivation causes oxidative stress and stimulates aggresome formation and autophagy in cultured cardiac myocytes. Biochim. Biophys. Acta 1802, 509–518.

Nagano, M., Suzuki, H., Ui-Tei, K., Sato, S., Miyake, T., Miyata, Y., 1998. H-7-induced apoptosis in the cells of a drosophila neuronal cell line through affecting unidentified H-7-sensitive substance(s). Neurosci. Res. 31, 113–121.

Saitoh, M., Ishikawa, T., Matsushima, S., Naka, M., Hidaka, H., 1987. Selective inhibition of catalytic activity of smooth muscle myosin light chain kinase. J. Biol. Chem. 262, 7796–7801.

Smith, U., Carvalho, E., Mosialou, E., Beguinot, F., Formisano, P., Rondinone, C., 2000. PKB inhibition prevents the stimulatory effect of insulin on glucose transport and protein translocation but not the antilipolytic effect in rat adipocytes. Biochem. Biophys. Res. Commun. 268, 315–320.

Smyth, J.T., Dehaven, W.I., Bird, G.S., Putney Jr., J.W., 2008. Ca2+-store-dependent and -independent reversal of Stim1 localization and function. J. Cell Sci. 121, 762–772.

Stathopulos, P.B., Ikura, M., 2017. Store operated calcium entry: from concept to structural mechanisms. Cell Calcium 63, 3–7.

Troncoso, R., Vicencio, J.M., Parra, V., Nemchenko, A., Kawashima, Y., Del Campo, A., Toro, B., Battiprolu, P.K., Aranguiz, P., Chiong, M., Yakar, S., Gillette, T.G., Hill, J.A., Abel, E.D., Leroith, D., Lavandero, S., 2012. Energy-preserving effects of IGF-1 antagonize starvation-induced cardiac autophagy. Cardiovasc. Res. 93, 320–329.

Uehara, A., Yasukochi, M., Imanaga, I., Nishi, M., Takeshima, H., 2002. Store-operated Ca2+ entry uncoupled with ryanodine receptor and junctional membrane complex in heart muscle cells. Cell Calcium 31, 89–96.

Voelkers, M., Salz, M., Herzog, N., Frank, D., Dolatabadi, N., Frey, N., Gude, N., Friedrich, O., Koch, W.J., Katus, H.A., Sussman, M.A., Most, P., 2010. Orai1 and Stim1 regulate normal and hypertrophic growth in cardiomyocytes. J. Mol. Cell. Cardiol. 48, 1329–1334.

Wang, Y.W., Zhang, J.H., Yu, Y., Yu, J., Huang, L., 2016. Inhibition of store-operated calcium entry protects endothelial progenitor cells from h2o2-induced apoptosis. Biomol. Ther. 24, 371–379.

Zhang, W., Trebak, M., 2011. STIM1 and Orai1: novel targets for vascular diseases? Sci. China Life Sci. 54, 780–785.

Zhang, L., Yu, J., Pan, H., Hu, P., Hao, Y., Cai, W., Zhu, H., Yu, A.D., Xie, X., Ma, D., Yuan, J., 2007. Small molecule regulators of autophagy identified by an image-based high-throughput screen. Proc. Natl. Acad. Sci. U. S. A. 104, 19023–19028.